

Aprotinin prevents proteolytic epithelial sodium channel (ENaC) activation and volume retention in nephrotic syndrome



Bernhard N. Bohnert^{1,2,3,7}, Martina Menacher^{1,7}, Andrea Janessa¹, Matthias Wörn¹, Anja Schork^{1,2,3}, Sophie Daiminger¹, Hubert Kalbacher⁴, Hans-Ulrich Häring^{1,2,3}, Christoph Daniel⁵, Kerstin Amann⁵, Florian Sure⁶, Marko Bertog⁶, Silke Haerteis⁶, Christoph Korbmacher⁶ and Ferruh Artunc^{1,2,3}

¹Department of Internal Medicine, Division of Endocrinology, Diabetology, Vascular Disease, Nephrology and Clinical Chemistry, University Hospital Tübingen, Tübingen, Germany; ²Institute of Diabetes Research and Metabolic Diseases (IDM) of the Helmholtz Center Munich at the Eberhards Karls University of Tuebingen, Tübingen, Germany; ³German Center for Diabetes Research (DZD) at the Eberhards Karls University of Tuebingen, Tübingen, Germany; ⁴Interfaculty Institute of Biochemistry, Eberhards Karls University of Tuebingen, Tübingen, Germany; ⁵Institute of Pathology, Friedrich-Alexander University Erlangen-Nürnberg (FAU), Erlangen, Germany; and ⁶Institute of Cellular and Molecular Physiology, Friedrich-Alexander University Erlangen-Nürnberg (FAU), Erlangen, Germany

Volume retention in nephrotic syndrome has been linked to activation of the epithelial sodium channel (ENaC) by proteolysis of its γ -subunit following urinary excretion of serine proteases such as plasmin. Here we tested whether pharmacological inhibition of urinary serine protease activity might protect from ENaC activation and volume retention in nephrotic syndrome. Urine from both nephrotic mice (induced by doxorubicin injection) and nephrotic patients exhibited high aprotinin-sensitive serine protease activity. Treatment of nephrotic mice with the serine protease inhibitor aprotinin by means of subcutaneous sustained-release pellets normalized urinary serine protease activity and prevented sodium retention, as did treatment with the ENaC inhibitor amiloride. In the kidney cortex from nephrotic mice, immunofluorescence revealed increased apical γ -ENaC staining, normalized by aprotinin treatment. In *Xenopus laevis* oocytes heterologously expressing murine ENaC, aprotinin had no direct inhibitory effect on channel activity but prevented proteolytic channel activation. Thus, our study shows that volume retention in experimental nephrotic syndrome is related to proteolytic ENaC activation by proteasuria and can be prevented by treatment with aprotinin. Hence, inhibition of urinary serine protease activity might become a therapeutic approach to treat patients with nephrotic-range proteinuria.

Kidney International (2018) **93**, 159–172; <http://dx.doi.org/10.1016/j.kint.2017.07.023>

KEYWORDS: aprotinin; ENaC; mice; nephrotic syndrome; protease inhibitor; proteolysis; proteolytic channel activation; serine protease

Correspondence: Ferruh Artunc, Department of Internal Medicine, Division of Endocrinology, Diabetology, Angiology and Nephrology, University Hospital of Tübingen, Otfried-Mueller-Strasse 10, 72076 Tübingen, Germany. E-mail: ferruh.artunc@med.uni-tuebingen.de

⁷MM and BNB share first authorship.

Received 11 March 2017; revised 24 July 2017; accepted 27 July 2017; published online 14 October 2017

Copyright © 2017, International Society of Nephrology. Published by Elsevier Inc. All rights reserved.

Nephrotic syndrome is characterized by proteinuria, edema, hypoalbuminemia, and hyperlipidemia; it is the most severe manifestation of proteinuric renal disease. The pathogenesis of edema formation in nephrotic syndrome remains debatable; both underfill and overfill theories have been proposed.¹ Studies in nephrotic rats have suggested that the distal tubule expressing the epithelial sodium channel (ENaC) is the site of sodium retention.² In addition to regulation by the mineralocorticoid hormone aldosterone,³ a special feature of ENaC is its complex post-translational regulation by proteases, which cleave specific sites in the extracellular domains of the α - and γ -subunits.⁴ Recent evidence suggests that proteolytic ENaC activation by urinary proteases may contribute to sodium retention in nephrotic syndrome.^{5,6} Protein-rich urine samples from both rats⁷ and patients⁸ who have nephrotic syndrome have been found to activate ENaC currents *in vitro*, presumably as a result of proteolysis of the γ -subunit of ENaC by serine proteases excreted in the urine.⁹ Currently, the serine protease plasmin has been implicated in promoting ENaC activation and volume retention during proteinuria.^{7,10} Plasmin cleaves the γ -subunit of ENaC at a distinct site and induces a robust increase in ENaC currents *in vitro*.^{10,11} In humans, a close correlation of urinary plasmin excretion with proteinuria has been found in preeclampsia⁸ and diabetic nephropathy.^{12,13} We have found a strong association of plasminuria with overhydration, as determined from bioimpedance spectroscopy in a large sample of patients with chronic kidney disease (CKD).¹⁴

Targeting urinary plasmin activity by pharmacologic inhibitors may be an interesting therapeutic approach, given the putative role of plasminuria in mediating volume retention and possibly podocyte injury.¹⁵ Plasmin can be inhibited by the serine protease inhibitor aprotinin, which competitively

interacts with its catalytic site, and by tranexamic acid, which inhibits plasminogen conversion into plasmin after occupying lysine-binding sites at the kringle domains of plasminogen. Camostat is an orally available serine protease inhibitor that is active against plasmin; it was originally developed in Japan for treatment of pancreatitis. Anecdotal reports suggest that camostat has beneficial effects in patients who have nephrotic syndrome.^{16,17} In addition, camostat has been reported to reduce blood pressure in salt-sensitive hypertensive rats, probably by preventing proteolytic ENaC activation, as suggested by the detection of partially but not fully cleaved γ ENaC.^{18,19} The inhibition of urinary plasmin activity requires the availability of these drugs in the tubular fluid. Aprotinin, as a small polypeptide with 58 amino acids (6.5 kDa), and tranexamic acid, as a water-soluble organic acid, are eliminated exclusively via glomerular filtration. Camostat is rapidly degraded by plasmatic esterases into 2 metabolites that are excreted in the urine, one of which has preserved inhibitory activity.²⁰ Therefore, these drugs, which have negligible plasma protein binding, can reach therapeutically relevant concentrations in the tubular fluid, making them candidates for a pharmacologic intervention to inhibit tubular protease activity in experimental nephrotic syndrome. Rats that have experimental heart failure and developed plasminuria, aprotinin treatment resulted in a blunted response to ENaC blockade by benzamil, suggestive of reduced ENaC activity.²¹

In this study, we tested the hypothesis that pharmacologic inhibition of urinary serine protease activity *in vivo* may reduce volume retention in nephrotic mice. Therefore, we used the inhibitors aprotinin, camostat, and tranexamic acid and tested their effect on volume retention in a model of experimental nephrotic syndrome developed by our group.^{22,23} We found that aprotinin treatment abolishes volume retention by preventing proteolytic ENaC activation.

RESULTS

Experimental nephrotic syndrome in mice features all the hallmarks of human nephrotic syndrome

Following a single injection of doxorubicin, mice with proteinuria exceeding 140 mg per mg creatinine developed nephrotic syndrome characterized by hypoalbuminemia (Figure 1a), body weight (BW) gain with ascites (Figure 1b; Supplementary Figure S1A), and hyperlipidemia evidenced by lipemic plasma (Supplementary Figure S1B). Although food and fluid intake remained fairly constant, except for a modest decrease during the initial days after doxorubicin treatment (Supplementary Figure S1C), urinary sodium/creatinine and urinary Na/K ratios dropped dramatically during the first 10 days, indicating that sodium retention caused the BW gain (Figure 1b; Supplementary Figure S1D). Urinary activity to cleave the amide bond of the chromogenic substrate S-2251 increased and was paralleled by a 1000-fold increase in urinary plasmin(ogen) excretion, as measured by both ELISA and a decrease in plasma plasmin(ogen) concentration (Figure 1c).

Urinary amidolytic activity was inhibited competitively *in vitro* by the serine protease inhibitors aprotinin (50% inhibitory concentration [IC₅₀] 56 [23; 137] nM) and camostat (IC₅₀ 2.4 [1.1; 4.9] μ M) but not by tranexamic acid (Figure 1d). Urinary amidolytic activity was also sensitive to inhibition by antiplasmin (IC₅₀ 51 [40; 66] nM), indicating that plasmin activity accounted for the vast proportion of urinary amidolytic activity against S-2251. Similar inhibition curves were obtained when amidolytic activity of purified plasmin was analyzed (Supplementary Figure S2). The IC₅₀ values were not significantly different (Supplementary Table S1), except for those for camostat (IC₅₀ 0.4 [0.4; 0.5] μ M, $P = 0.0003$).

Patients who have nephrotic syndrome display aprotinin-sensitive urinary serine protease activity

In 10 patients with acute nephrotic syndrome and nephrotic-range proteinuria (as characterized in Supplementary Table S2 and by Schork *et al.*¹⁴), we detected strong urinary amidolytic activity that was almost absent in 15 healthy subjects (Figure 2a and b; Supplementary Table S2). In nephrotic patients, this activity was largely sensitive to aprotinin and accounted for 73% \pm 7% of total activity, whereas this proportion was only 10% \pm 3% in healthy subjects ($P < 0.0001$). The increased urinary amidolytic activity in the nephrotic patients paralleled the expansion of extracellular volume, as quantified by bioimpedance spectroscopy (Figure 2c; Supplementary Table S2). These findings confirm that nephrotic syndrome in both humans and mice leads to excretion of urinary serine proteases that might be involved in volume retention.

Treatment of nephrotic mice with aprotinin prevents volume retention

To test the effect of pharmacologic inhibition of urinary serine protease activity *in vivo*, we treated 3 groups of nephrotic mice with aprotinin, camostat, and tranexamic acid, respectively, delivered by sustained-release pellets. After inducing nephrotic syndrome, we implanted the pellets subcutaneously on day 3 and followed nephrotic mice until day 10. Nephrotic mice given placebo pellets served as controls. After induction of nephrotic syndrome, the level of proteinuria (Figure 3a) as well as food and fluid intake was similar in all treatment groups (Supplementary Figure S3A and B). Urinary amidolytic activity was suppressed by aprotinin but not by camostat or tranexamic acid (Figure 3b). Although camostat and tranexamic acid-treated nephrotic mice had BW gain similar to that of placebo-treated nephrotic mice, aprotinin-treated nephrotic mice were protected from BW gain (Figure 3c). Accordingly, the urinary sodium/creatinine ratio was normalized in aprotinin-treated nephrotic mice compared with the other groups (Figure 3d; Supplementary Figure S3C). Treatment with aprotinin prevented the reduction in plasma sodium concentration seen in the other nephrotic groups (Table 1). Compared with healthy mice, nephrotic mice of all groups tended to have higher plasma

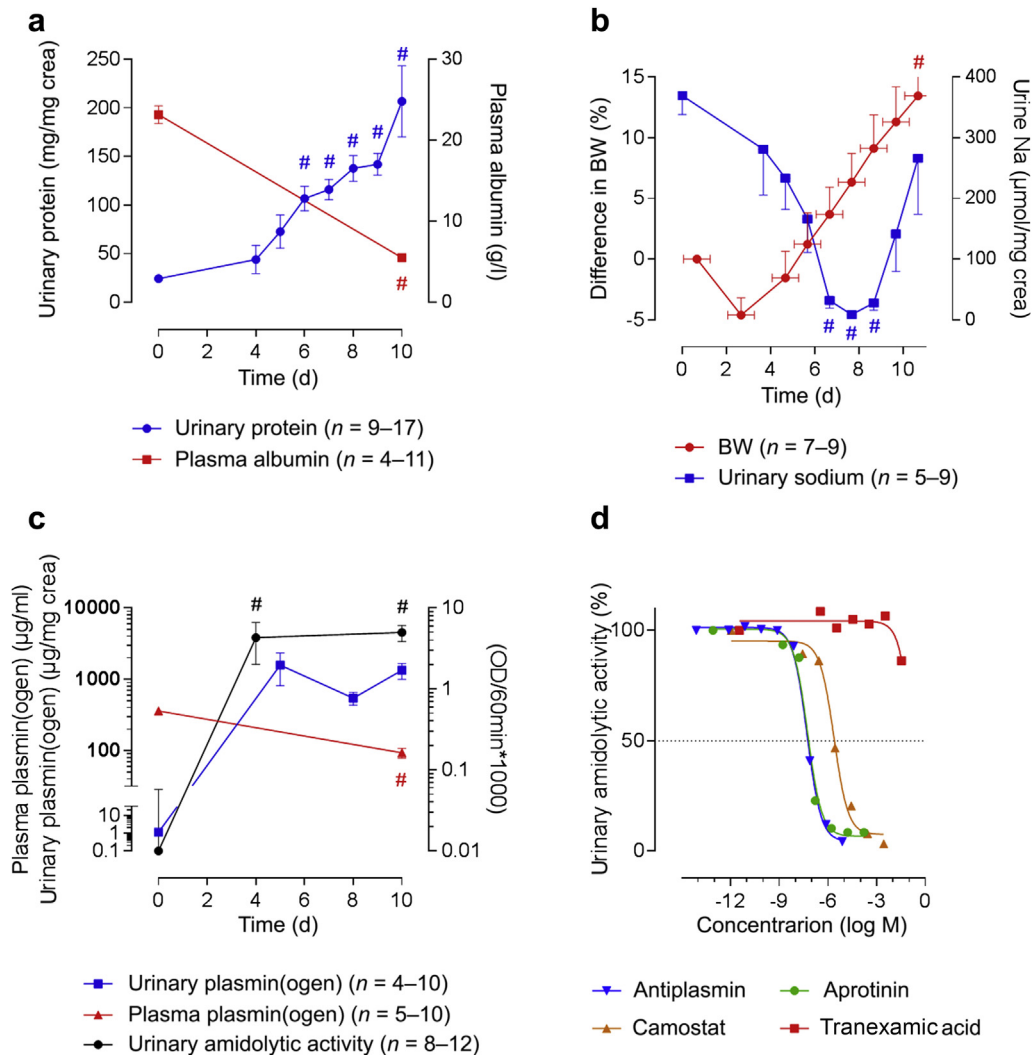


Figure 1 | Characteristics of experimental nephrotic syndrome in 129S1/SvlmJ mice. After a single doxorubicin dose, all hallmarks of human nephrotic syndrome were present, including proteinuria and hypoalbuminemia (a), body weight (BW) gain, and urinary sodium retention (b). Proteinuria was paralleled by urinary amidolytic activity against S-2251 and urinary plasmin(ogen) excretion, leading to a decrease in plasma plasmin(ogen) concentration (c). Inhibition curves for amidolytic activity in nephrotic urine (d). Pooled curve from $n = 5-7$ single curves with final concentration of urinary protein between 4000 and 6000 $\mu\text{g}/\text{ml}$. Arithmetic means \pm SEM. #Significant difference to baseline value. d, day; min, minute; M, molarity; OD, optical density.

potassium concentrations and to be hypoalbuminemic (Table 1). The glomerular filtration rate, as estimated from plasma urea and creatinine concentrations, was mildly reduced in nephrotic mice, with the difference, compared with healthy mice, reaching statistical significance in mice treated with tranexamic acid (Table 1).

Urinary and plasma aprotinin concentrations under treatment with 1 mg of aprotinin per day are shown in Figure 3e. The mean urinary aprotinin concentration was $443 \pm 90 \mu\text{g}/\text{ml}$ ($68 \pm 13 \mu\text{M}$), whereas the plasma aprotinin concentration after 10 days of treatment was $14 \pm 2 \mu\text{g}/\text{ml}$ ($2.1 \pm 0.3 \mu\text{M}$), comparable to the plasma concentration achieved in aprotinin-treated patients.²⁴ Dose–response studies with various aprotinin doses found that 0.5 mg per day and 1 mg per day partially and completely, respectively, prevented BW gain, although urinary amidolytic activities (both *in vitro* and *in vivo*) were

inhibited by lower doses, such as 0.25 mg per day and 0.5 mg per day (Figure 3f). Similar effects to those found with aprotinin were obtained after treatment with the ENaC blocker amiloride, which also prevented sodium retention and BW gain in nephrotic mice (Figure 4a, b, and c). This finding confirms the concept that increased ENaC-mediated sodium absorption plays a major role in volume retention in nephrotic syndrome and suggests that the therapeutic effect of aprotinin is mediated by inhibition of proteolytic ENaC activation by urinary serine proteases.

Plasma aldosterone is reduced by aprotinin and is not essential for volume retention

Compared with those in healthy mice, plasma aldosterone concentrations were higher in nephrotic mice on placebo treatment but not in nephrotic mice treated with aprotinin,

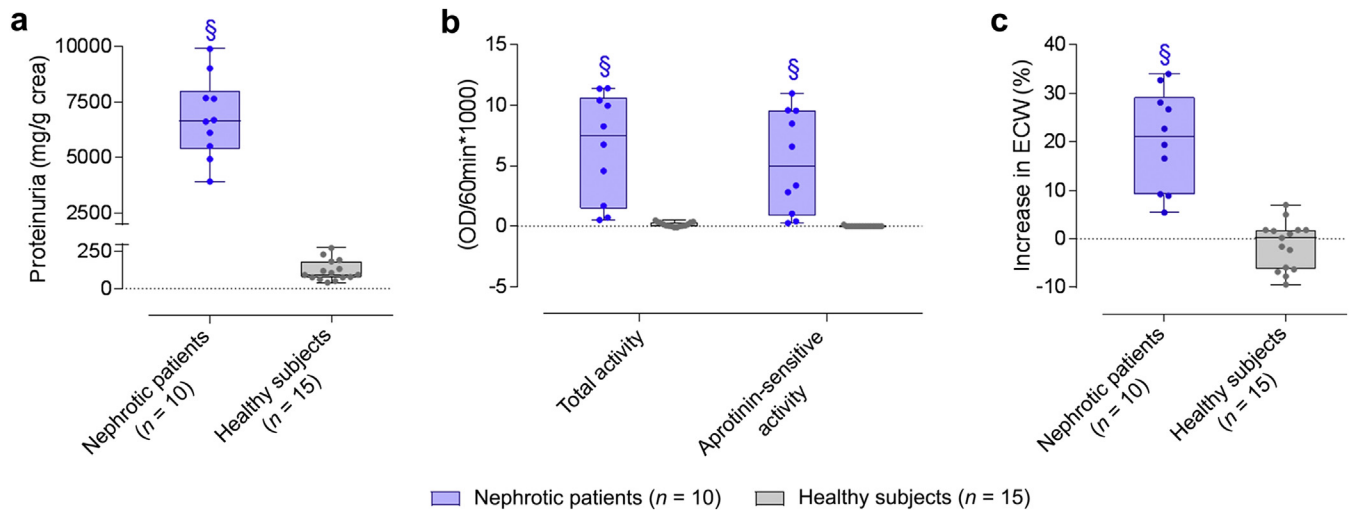


Figure 2 | Aprotinin-sensitive proteasuria and overhydration in nephrotic patients. Urine samples from patients with nephrotic syndrome exhibit high proteinuria (a) and urinary serine protease activity that is sensitive to aprotinin (b). This is paralleled by massive overhydration, as assessed with bioimpedance spectroscopy (c). Optical density (OD) is measured at 405 nm. §Significant difference between healthy subjects and nephrotic patients. ECW, extracellular water.

camostat, or tranexamic acid (Figure 4d). To determine the contribution of hyperaldosteronism and exclude the possibility that the effect of aprotinin was due to prevention of hyperaldosteronism, we studied volume retention under suppressed aldosterone secretion and mineralocorticoid receptor (MR) blockade. Compared with nephrotic mice on a normal diet, those on a high-salt diet had significantly greater BW gain (+33.0% ± 6.4%), despite a suppressed aldosterone plasma concentration. Still, aprotinin treatment inhibited volume retention in mice with high-salt intake (Supplementary Figure S4A). Treatment with the MR blocker potassium canrenoate did not prevent volume retention, although the increase tended to be slightly blunted (+15.9% ± 3.3%; Figure 4a, b, and c). As shown in Supplementary Figure S4B, maximal BW gain did not parallel plasma aldosterone concentration during various treatments, evidence against a major and causal contribution of aldosterone to the observed volume retention. Quantitative polymerase chain reaction testing revealed that nephrotic mice had significantly increased renin transcript levels, compared with healthy mice, whereas these levels were suppressed in aprotinin-treated nephrotic mice (Figure 4e). The results were robust when mRNA transcript levels were expressed in absolute copies or normalized to β-actin (Supplementary Figure S5A and B). Glyceraldehyde-3-phosphate dehydrogenase (GAPDH) was significantly less expressed in aprotinin-treated nephrotic mice and therefore could not be used for normalization (Supplementary Figure S5C).

Aprotinin treatment affects expression of γ-ENaC and its cleavage products

Compared with healthy mice, mRNA expression of the α-, β-, and γ-subunits of ENaC tended to be lower in placebo-treated nephrotic mice, a difference that reached statistical significance in aprotinin-treated nephrotic mice (Figure 5a; Supplementary

Figure S6A and B). Analysis of the γ-ENaC expression in renal cortical tissue by Western blotting using a C-terminal mouse γ-ENaC antibody revealed multiple bands at 44, 53, 70, 76, and 86 kDa that were blocked by the application of the immunogenic peptide (Figure 5b). Linearity of the signal intensity was confirmed with different loading (Supplementary Figure S7A and B). The strongest band among these was the one at 70 kDa, most likely representing furin-cleaved γ-ENaC at the plasma membrane; the 86-kDa band represented full-length γ-ENaC (Figure 5c). However, a specific band representing extracellularly cleaved γ-ENaC, which is expected to be 5 kDa smaller than furin-cleaved γ-ENaC, was not detectable. Compared with healthy mice, the expression of the bands at 53, 70, 76, and 86 kDa was significantly decreased in placebo-treated nephrotic mice. A similar pattern was observed in aprotinin-treated nephrotic mice; however, the band at 53 kDa was significantly decreased compared with that in healthy and placebo-treated nephrotic mice (Figure 5e).

Histologic analysis of renal tissue revealed up-regulation of γ-ENaC stain in placebo-treated nephrotic mice (Figure 6), resulting in a significantly higher staining score compared with that of healthy mice (1.8 ± 0.03 vs. 0.9 ± 0.04, P = 0.0004; Supplementary Figure S8A). At higher magnification, increased staining was observed, particularly at the luminal side of the principal cells, similar to previous findings in nephrotic rats and termed apical targeting of ENaC.²⁵ Aprotinin treatment normalized γ-ENaC staining (0.8 ± 0.1) and prevented apical targeting. Staining with γ-ENaC was negative in the presence of the blocking peptide (Supplementary Figure S8B).

Aprotinin has no inhibitory effect on ENaC activity and prevents the appearance of a γ-ENaC cleavage product at 67 kDa in *Xenopus laevis* oocytes

Based on the similar efficacy of the ENaC blocker amiloride and the serine protease inhibitor aprotinin, we further

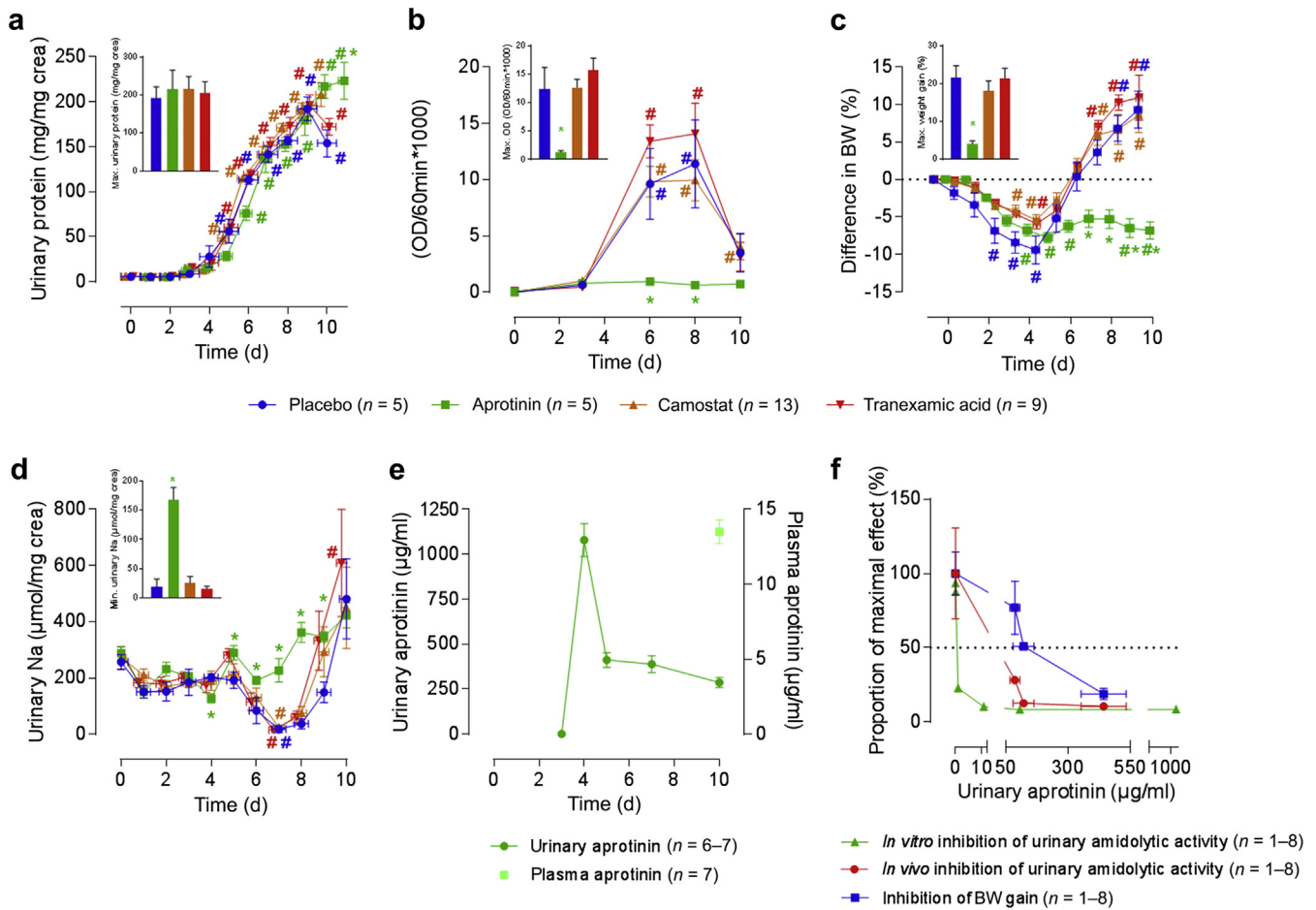


Figure 3 | Treatment of nephrotic mice with aprotinin, camostat, and tranexamic acid. Course of proteinuria (a; inset: maxima [max.]), urinary amidolytic activity (b, inset: max.), body weight (BW) (c; inset: max.) and urinary sodium/creatinine ratio (d; inset: minima [min.]) in nephrotic mice treated with placebo, aprotinin, camostat, or tranexamic acid. Urinary and plasma aprotinin concentration during treatment with 1 mg/d aprotinin (e) and dose–response curves showing the relationship between urinary aprotinin concentration and inhibition of amidolytic activity (*in vitro* and *in vivo*, respectively) and maximal (BW) gain (f). Arithmetic means \pm SEM. #Significant difference from baseline value, *Significant difference between aprotinin- and placebo-treated mice. d, day.

analyzed the mode of action of aprotinin by studying its effect on murine ENaC heterologously expressed in *Xenopus laevis* oocytes. As shown in Figure 7a, b, and c, application of 500 μ g/ml aprotinin—a concentration achieved in the urine of aprotinin-treated nephrotic mice—to the bath solution did not markedly affect ENaC-mediated currents. The minor

current rundown observed with aprotinin was similar to that observed in time-matched control experiments with mock solution exchange (Figure 7b and c). These results exclude a relevant direct inhibitory effect of aprotinin on ENaC.

In additional control experiments, the prototypical serine protease chymotrypsin (2 μ g/ml) increased amiloride-sensitive

Table 1 | Plasma values after 10 days of treatment with aprotinin, camostat, and tranexamic acid in nephrotic mice

Parameter	Healthy mice	Nephrotic mice treatment			
		Placebo	Aprotinin	Camostat	Tranexamic acid
Plasma Na (mM)	152 \pm 1	145 \pm 1 [#]	148 \pm 1	145 \pm 1 [#]	145 \pm 1 [#]
Plasma K (mM)	4.3 \pm 0.1	4.7 \pm 0.1	5.0 \pm 0.2	4.9 \pm 0.1 [#]	5.0 \pm 0.1 [#]
Plasma bicarbonate (mM)	22 \pm 1	27 \pm 1	28 \pm 1 [#]	28 \pm 1 [#]	28 \pm 1 [#]
Venous pH	7.31 \pm 0.01	7.36 \pm 0.01 [#]	7.37 \pm 0.01 [#]	7.37 \pm 0.01 [#]	7.36 \pm 0.01 [#]
Plasma urea (mg/dl)	34 \pm 2	35 \pm 12	63 \pm 16	52 \pm 13	31 \pm 5
Plasma creatinine (mg/dl)	0.24 \pm 0.03	0.61 \pm 0.14	0.44 \pm 0.12	0.49 \pm 0.09	0.74 \pm 0.19 [#]
Plasma albumin (g/l)	20.3 \pm 0.2	6.7 \pm 0.3 [#]	7.5 \pm 0.7 [#]	7.0 \pm 0.6 [#]	6.8 \pm 0.4 [#]

Arithmetic means of n = 4–12 mice per group \pm SEM. #indicates a significant difference compared with healthy mice.

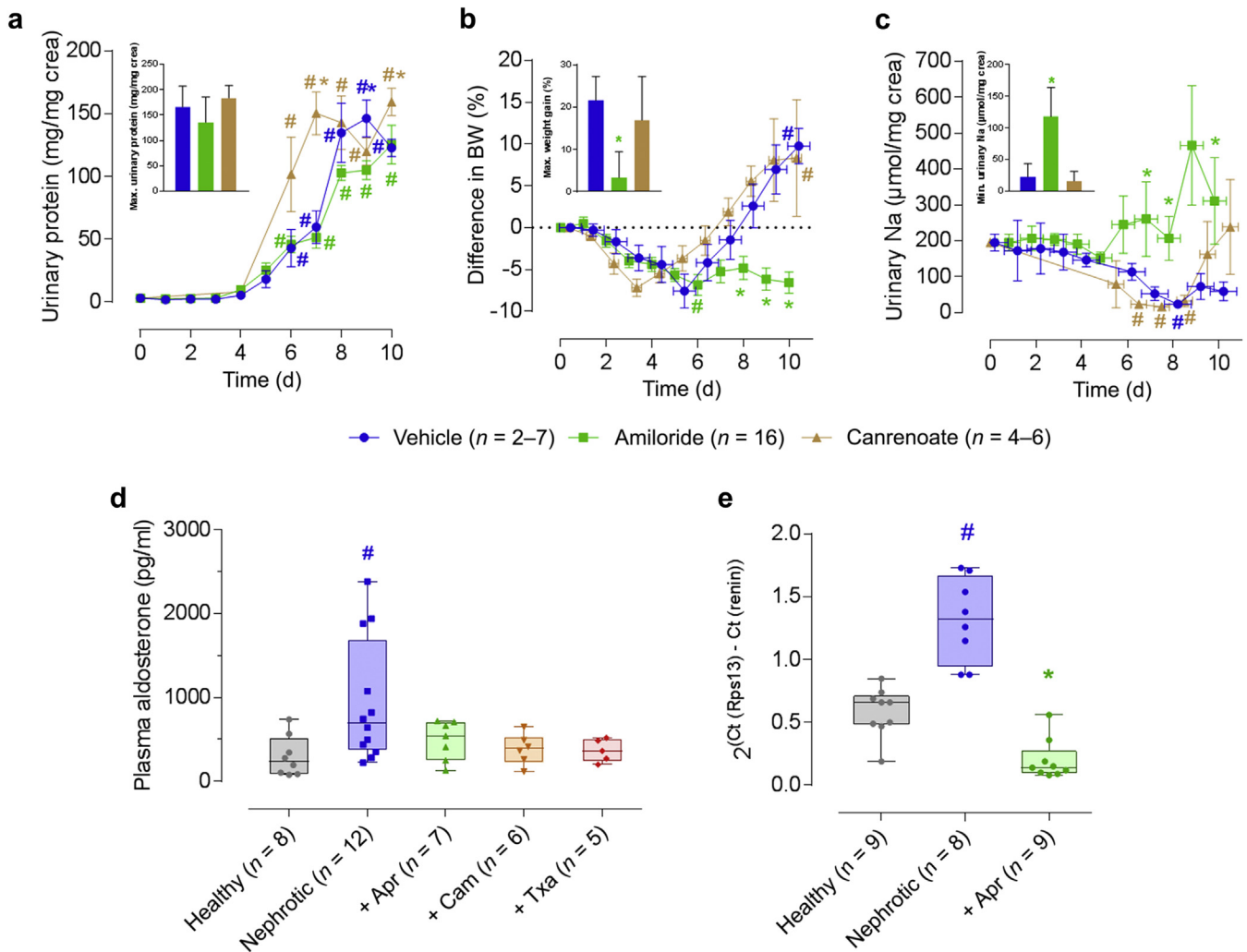


Figure 4 | Effect of amiloride and canrenoate treatment in nephrotic mice, and the role of plasma aldosterone. Course of proteinuria (a; inset: maxima [max.]), body weight (BW; b; inset: max.) and urinary Na excretion (c; inset: minima [min.]) in nephrotic mice treated with vehicle, amiloride (10 μg/g i.p.), or canrenoate (400 mg/l in drinking water; average intake 95 μg/g). Urine was collected 4 hours after injection of vehicle or amiloride. Plasma aldosterone concentration during treatment with serine protease inhibitors (d) as well as transcript levels of renin (e) in healthy, placebo-treated, and aprotinin-treated nephrotic mice normalized to the housekeeping gene *Rps13* in healthy, placebo-treated, and aprotinin-treated nephrotic mice ($n = 8-9$ each). Arithmetic means \pm SEM. #Significant difference from baseline value (a-c) or healthy mice (d,e); *significant difference between placebo and amiloride-treated nephrotic mice (a-c), or between placebo- and aprotinin-treated nephrotic mice (e). apr, aprotinin; cam, camostat; Ct, cycle threshold; d, day; txa, tranexamic acid.

ENaC-mediated whole-cell currents approximately 2-fold (Supplementary Figure S9A). In this concentration, chymotrypsin has been found to fully activate ENaC by cleaving the channel at a specific site in its γ -subunit.¹¹ Subsequent addition of 500 μg/ml aprotinin to the chymotrypsin-containing solution did not affect ENaC-mediated currents (Supplementary Figure S9B). Application of chymotrypsin in the presence of aprotinin failed to stimulate ENaC currents, whereas subsequent removal of aprotinin in the continuous presence of chymotrypsin revealed the expected ~2-fold proteolytic ENaC activation (Supplementary Figure S9C). In parallel Western blots assessing biotinylated cell surface-expressed γ -ENaC (Figure 7d), a predominant cleavage product of ~76 kDa was detectable in oocytes expressing $\alpha\beta\gamma$ -ENaC. In the oocyte system, full-length mouse γ -ENaC migrates at ~87 kDa and is

readily detectable in whole-cell lysate or in membrane-enriched fractions but usually not at the cell surface.^{7,11,26} This finding indicates that γ -ENaC detected at the plasma membrane is pre-cleaved at amino acid position 143 by the endogenous serine protease furin, which is not sensitive to aprotinin²⁷ (Figure 5c). As expected, ENaC activation by chymotrypsin treatment induced a shift of the molecular size of cell surface-expressed γ -ENaC, from 76 to 67 kDa (Figure 5c). This finding supports the concept that a second cleavage event in γ -ENaC is required as a final step in proteolytic channel activation.¹¹ The appearance of the ~67-kDa cleavage fragment was prevented when chymotrypsin was applied in the presence of aprotinin (Figure 7d), consistent with the finding that aprotinin prevented the activation of ENaC currents by chymotrypsin (Supplementary Figure S9C). Aprotinin

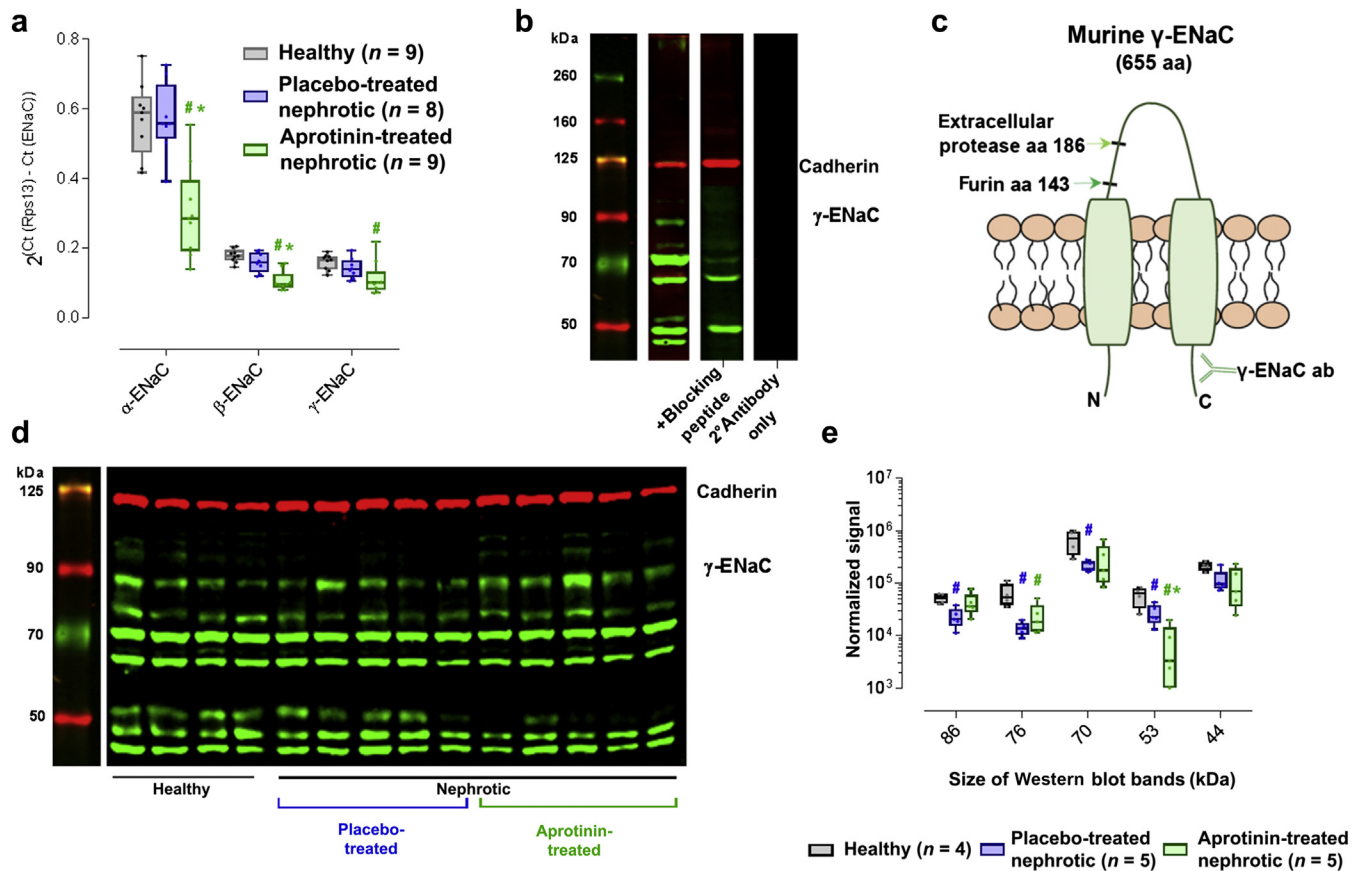


Figure 5 | Expression of γ -epithelial sodium channel (γ -ENaC) in renal cortex. Relative mRNA expression of the α -, β -, and γ -subunit of ENaC in healthy, placebo-treated nephrotic, and aprotinin-treated nephrotic mice, normalized to the housekeeping gene *Rps13*, which had constant expression across the groups ($n = 8$ – 9 each; **a**). Western blot from renal cortex revealing several bands between 44 and 86 kDa. Administration of the blocking peptide attenuated bands at 44, 53, 70, 76, and 86 kDa, whereas bands at 65 and 48 kDa were not blocked (**b**). γ -ENaC contains 2 cleavage sites within the pore-forming loop for posttranslational proteolytic processing. At amino acid (aa) position 143, γ -ENaC is cleaved intracellularly by the serine protease furin, and at aa 186 extracellularly in the tubulus lumen by an extracellular serine protease. The molecular weights of full-length and furin-cleaved γ -ENaC are 15 kDa apart, and those between furin and extracellularly cleaved γ -ENaC are 5 kDa apart, as detected by an antibody against the C terminus of γ -ENaC (**c**). (**d**) Western blots from membrane proteins of healthy, placebo-treated nephrotic and aprotinin-treated nephrotic mice. Cadherin expression at 125 kDa served as a loading control. (**e**) Relative abundance of the 44, 53, 70, 76 and 86 kDa bands in healthy, placebo-treated nephrotic, and aprotinin-treated nephrotic mice normalized to the cadherin expression. #Significant difference from healthy mice; * indicates a significant difference between placebo- and aprotinin-treated nephrotic mice. ab, antibody; Ct, cycle threshold.

treatment alone had no effect on the appearance of the ~ 76 -kDa fragment. We also tested the long-term effect of aprotinin on ENaC currents. Pre-incubation of murine ENaC-expressing oocytes for 48 hours in aprotinin had no significant effect on baseline ENaC-mediated currents and did not alter the relative stimulatory effect of chymotrypsin (Supplementary Figure S9D).

DISCUSSION

This study is the first to reveal the pathophysiological role of urinary serine protease activity and proteolytic ENaC activation for volume retention in an *in vivo* model of experimental nephrotic syndrome. The findings highlight that treatment with the serine protease inhibitor aprotinin abolished ENaC-mediated sodium retention by preventing proteolytic ENaC activation. However, whether this effect is related to inhibition of plasmin or whether other aprotinin-sensitive serine

proteases contribute to or mediate this effect is unclear. These other serine proteases might include membrane-anchored prostatic and tissue kallikreins that are involved in the physiological regulation of ENaC,^{28,29} as well as serine proteases of the coagulation cascade that are aberrantly filtered during proteinuric disease. Also unclear is whether complex serine protease cascades are involved in proteolytic ENaC activation. For example, plasmin may activate ENaC by direct cleavage at a distinct site¹¹ or may activate prostatic that subsequently cleaves γ -ENaC at the putative prostatic site.³⁰ Aprotinin also inhibits prostatic with high affinity (IC_{50} 1.8 nM³¹); thus, the efficacy of aprotinin may result from the inhibition of both pathways. Further studies are needed to elucidate the complex mechanisms of proteolytic ENaC activation during nephrotic syndrome and the effect of aprotinin.

In our study, patients who had acute nephrotic syndrome, and nephrotic mice, revealed volume retention and excretion

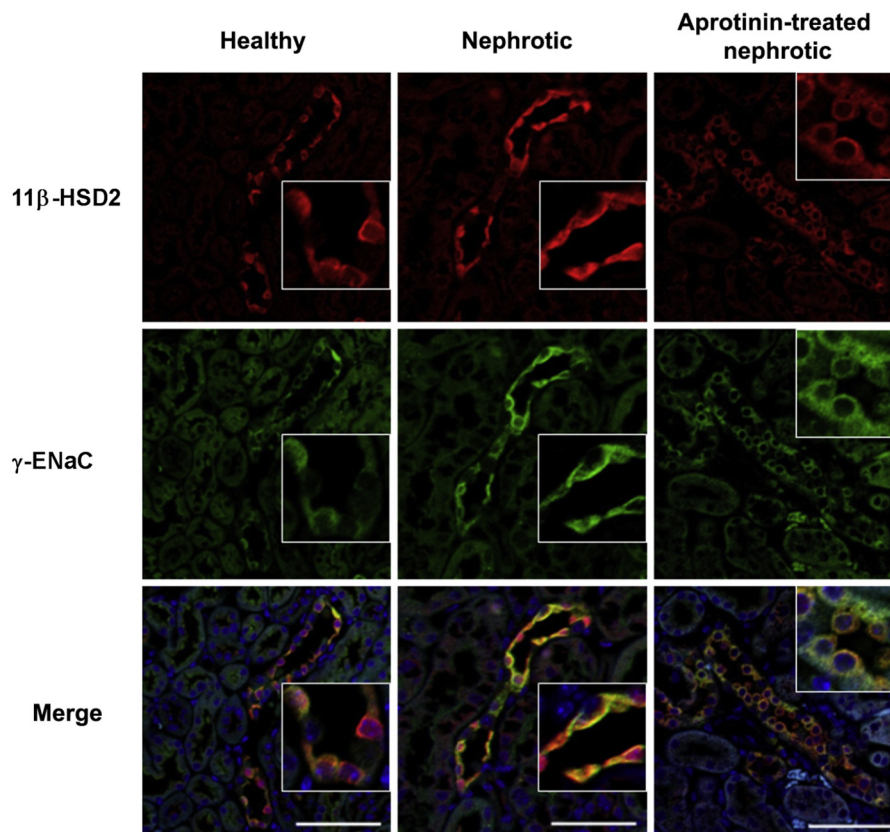


Figure 6 | Histologic expression of γ -epithelial sodium channel (γ -ENaC) in the aldosterone-sensitive distal nephron.

Immunofluorescence of fixed kidney sections from healthy and nephrotic mice treated with placebo or aprotinin at 200-fold magnification (bar = 50 μ m). Inset: 630-fold magnification corresponding to 28 x 28 μ m. Antibodies are directed against γ -ENaC (green) and 11 β -hydroxysteroid dehydrogenase type 2 (HSD-2; red) defining the distal nephron. Nuclei are stained blue with 4e,6-diamidino-2-phenylindole. To optimize viewing of this image, please see the online version of this article at www.kidney-international.org.

of aprotinin-sensitive serine proteases in the urine, which can be termed proteasuria. This finding suggests common mechanisms in ENaC activation of nephrotic patients and the current nephrotic mouse model, supporting the model's validity for studying human disease. Currently, plasmin is suggested to be the principal serine protease involved in ENaC-mediated sodium retention in nephrotic syndrome.^{5,7} However, the possibility remains that aprotinin-sensitive serine proteases other than plasmin are involved. Our findings are a proof of principle of inhibition of urinary serine protease activity as a potential new therapeutic approach that could be translated into clinical medicine to treat nephrotic patients. Compared with direct ENaC blockade with the diuretic amiloride, the inhibition of excessive urinary serine protease activity could protect against ENaC-mediated volume retention while minimally interfering with basal ENaC function. Therefore, this approach might confer protection from development of life-threatening hyperkalemia, which limits amiloride treatment in clinical practice, particularly in patients who have renal insufficiency.^{32–35} Notably, plasma potassium concentration was not higher in aprotinin-treated nephrotic mice compared with placebo-treated nephrotic mice. Although it was effective in this study, aprotinin might

not be an ideal drug for treatment of patients, owing to its adverse effects, including renal events.³⁶

Western blot analyses from mouse kidneys and oocytes expressing murine ENaC revealed distinct differences in the expression of the γ -ENaC cleavage products. In plasma membranes from oocytes, γ -ENaC was only expressed at 76 kDa, and the addition of chymotrypsin induced a shift to 67 kDa, corresponding to extracellularly cleaved γ -ENaC. In contrast, healthy mice expressed multiple bands under control conditions; the bands at 86 and 70 kDa, respectively, probably represented full-length and furin-cleaved γ -ENaC. Although the appearance of serine proteases is expected to result in proteolytic activation of γ -ENaC *in vivo*, we could not clearly detect a band with the expected size that could represent extracellularly cleaved γ -ENaC, except for a band at 53 kDa that was attenuated by aprotinin treatment. However, γ -ENaC fragments lower than 65 kDa have not been found to represent proteolytically activated ENaC. In similar Western blots analyses from mouse kidney homogenates using an analogous antibody directed against the corresponding C-terminal γ -ENaC sequence from rat, Yang *et al.*³⁷ detected bands at 80, 70, and 65 kDa, with the latter presumed to represent extracellularly cleaved γ -ENaC. The reason for the

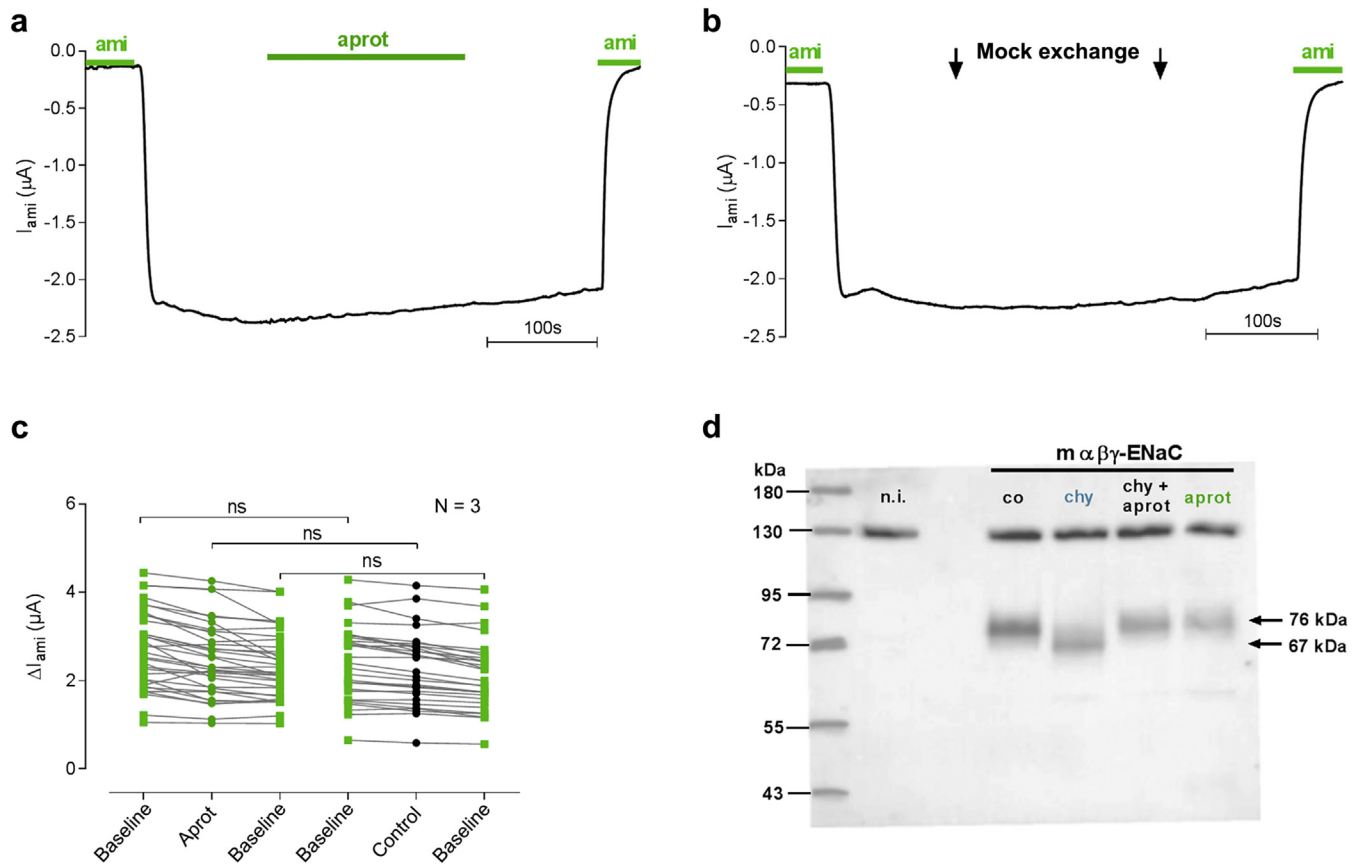


Figure 7 | Aprotinin (aprot) has no inhibitory effect on epithelial sodium channel (ENaC) activity and prevents the appearance of a γ -ENaC cleavage product at 67 kDa. Representative whole-cell current traces from oocytes expressing murine ENaC. Amiloride (ami; 2 μ M) or aprot (500 μ g/ml) were present in the bath solution as indicated (**a,b**). Summary of similar experiments as shown in (**a,b**). Data points obtained from individual oocytes are connected by a line (**c**). Expression of biotinylated γ -ENaC at the cell surface, analyzed by sodium dodecylsulfate polyacrylamide gel electrophoresis. Oocytes expressing murine ENaC were preincubated for 30 minutes in protease-free control solution (co), or in a solution containing chymotrypsin (chy), chy + aprot, or aprot. γ -ENaC was detected with an antibody against the C terminus of murine γ ENaC. This antibody detected an unspecific band of \sim 130 kDa that was also present in non-injected (n.i.) oocytes (**d**). N indicates the number of different batches of oocytes. ns, nonsignificant.

difference in molecular weight of this γ -ENaC cleavage product found in our study versus that of Yang *et al.*³⁷ is unclear and might be related to differences in one or more of the total of five N-glycosylation sites,³⁸ the sample preparation, and/or the antibody used. Also, the process of fluorescence detection using infrared dye-labelled antibodies is far more sensitive than the commonly employed process of chemiluminescence detection. Western blot analysis from whole kidney homogenates, as a means to assess ion channels, is inherently limited by difficulty in distinguishing between cell-surface and intracellularly expressed ion channels. To overcome this limitation, the group of Palmer has developed a protocol has been developed to analyze cell surface-expressed ENaC using *in vivo* biotinylation.^{39,40} Although this approach has been successfully implemented in rats, we chose to enrich membrane proteins using ultracentrifugation. We also employed a blocking peptide to delineate unspecific bands seen at 48 kDa and 65 kDa. In this respect, histologic analysis is more suitable for analyzing expression of functionally active channels at the plasma membrane. Immunofluorescence

revealed marked up-regulation of γ -ENaC staining, particularly at the apical side, in placebo-treated nephrotic mice, an effect that might be related to increased apical targeting due to hyperaldosteronism.^{25,41} Aprotinin inhibited apical targeting, most likely via suppression of hyperaldosteronism. Due to the used antibody, immunofluorescence does not allow for any inferences to be drawn regarding γ -ENaC proteolysis.

Our electrophysiological data using mouse ENaC-expressing oocytes clearly reveal that aprotinin does not exert a direct inhibitory effect on ENaC *in vitro* but does prevent its proteolytic activation and the appearance of the 67-kDa γ -ENaC cleavage fragment representing the fully active channel. This finding is consistent with previous findings from Carattino *et al.*²⁸ in ENaC-expressing oocytes, and with results reported by Jacquillet *et al.*⁴² revealing that aprotinin abolished the stimulatory effect of chymotrypsin on sodium reabsorption *in vivo*, whereas aprotinin alone had no effect.

Although activation of renin and aldosterone secretion was suppressed in all mice treated with serine protease inhibitors, only aprotinin-treated mice were protected from the increase

in amidolytic activity and volume retention. This finding might be the result of insufficient delivery of camostat and tranexamic acid to the distal tubule. A study with radiolabeled camostat found that only 12% of the radioactivity found in urine corresponded to the active metabolite 4-(4-guanidino benzoyloxy)-phenyl acetic acid methanesulfonate (GBPA).²⁰

Our findings support the overfill hypothesis of sodium retention during nephrotic syndrome, in several respects. First, the onset of sodium retention occurred immediately after proteinuria began. Second, the proteinuria had to be in excess of approximately 140 mg/mg crea to induce sodium retention. This points to proteins that are aberrantly filtered when glomerular permeability greatly increases and is similar to characteristics of nephrotic syndrome in humans, which has a threshold of >3.5 g per day. Third, sodium retention was completely abolished by the serine protease inhibitor aprotinin, which is not a diuretic and does not directly block ENaC like amiloride. Fourth, volume retention was not directly related to plasma aldosterone concentration and occurred in aldosterone-suppressed or even aldosterone-blocked conditions. This finding is in agreement with results of studies examining the role of hyperaldosteronism in experimental nephrotic syndrome in adrenalectomized rats with aldosterone deficiency⁴³ and in aldosterone-resistant mice lacking the serum and glucocorticoid kinase 1 (SGK1), conducted by our group.²² However, hyperaldosteronism might contribute to volume retention in experimental nephrotic models by stimulating ENaC production.^{25,41} This murine model contains elements of both the overfill and underfill hypotheses of edema formation,^{1,6} but sodium retention was primarily caused by proteolytic ENaC activation and followed by underfill due to severe hypoalbuminemia. Our study reveals that aprotinin is a potent drug to address both of these elements by preventing excessive proteolytic ENaC activation as well as hyperaldosteronism.

METHODS

Animals

Experiments were performed on 3-month-old wild-type 129 S1/SvImJ mice purchased from The Jackson Laboratory (Bar Harbor, ME). Mice were kept on a 12:12-hour light–dark cycle and fed a standard diet (sodium content 0.24%, corresponding to 104 $\mu\text{mol/g}$; ssniff Spezialdiaeten, Soest, Germany) with tap water *ad libitum*. Experimental nephrotic syndrome was induced after a single i.v. injection of doxorubicin (14.5 $\mu\text{g/g}$ BW; Cell Pharm, Bad Vilbel, Germany). Mice were kept individually in their usual cages, to reduce distress after doxorubicin injection, pellet implantation, and proteinuria. Samples of spontaneously voided urine were collected in the morning, 2 days before (baseline) and up to 10 days after doxorubicin injection. Daily food and fluid intake was monitored. Blood samples were drawn before induction and at sacrifice on day 10. [Supplementary Table S3](#) depicts the number of included mice and excluded/dead mice.

Treatments were performed using custom-made subcutaneous pellets with matrix-driven sustained release (Innovative Research of America, Sarasota, FL). Pellets were implanted subcutaneously on the backs of the mice on day 3 after doxorubicin injection. The optimal doses, chosen after conducting dose-finding studies, were

1 mg per day for bovine aprotinin (6000 KIU/mg, LOXO, Heidelberg, Germany), 1.5 mg per day for camostat (kindly donated by Ono Pharmaceutical Co., Osaka, Japan), and 2 mg per day for tranexamic acid (Sigma-Aldrich, Munich, Germany). We did not encounter any local problems with the pellets. Amiloride was administered i.p. at a dose of 10 $\mu\text{g/g}$, once daily. To study the role of aldosterone in volume retention, we used a high-salt intake (1% in drinking water) to suppress aldosterone secretion, and potassium canrenoate to block aldosterone action (400 mg/l in drinking water)⁴⁴ in a subgroup of animals.

Patients

Spot urine samples were obtained from patients treated for acute nephrotic syndrome at University Hospital Tübingen between September 2012 and April 2013.¹⁴ Subjects evaluated for living, related kidney transplantation were included as healthy controls. All human samples were obtained after informed consent. Fluid status was assessed by bioimpedance spectroscopy measurements using a body composition monitor (Fresenius Medical Care, Bad Homburg, Germany). Urinary amidolytic activity was determined using the chromogenic substrate S-2302, which is a substrate of serine proteases (Haemochrom Diagnostica, Essen, Germany). A sample of 50 μl of urine was incubated with 2 mM S-2302 for 8 hours, at 37 °C, with and without aprotinin (0.11 mg/ml). The difference in optical density at 405 nm between these 2 conditions reflected the aprotinin-sensitive serine protease activity.

Laboratory assays

Plasma urea and creatinine, as well as urinary creatinine, were measured with a colorimetric assay (Labor + Technik Eberhard Lehmann, Berlin, Germany); plasma electrolytes and bicarbonate were measured using a GEM Premier 3000 blood gas analyzer (Instrumentation Laboratory, Munich, Germany). Urinary protein concentration was quantified using the Bradford method (Bio-Rad Laboratories, Munich, Germany); urinary sodium concentration was quantified with flame photometry (EFUX 5057, Eppendorf, Hamburg, Germany). Both urinary protein and sodium concentration were normalized to the urinary creatinine concentration. Plasma aldosterone was measured using an ELISA kit (IBL International, Hamburg, Germany); plasma albumin was measured using a fluorometric kit, against mouse albumin as a standard (Progen Biotechnik, Heidelberg, Germany). Urinary amidolytic and plasmin activity was determined by incubating 3 μl urine or purified active plasmin (Merck, Darmstadt, Germany) with the chromogenic substrate S-2251 (Haemochrom Diagnostica, Essen, Germany), at 37 °C, for 1 hour. Amidolytic activity was calculated from the change in UV absorption at 405 nm. Inhibition curves were generated with serial dilution of aprotinin, camostat, tranexamic acid, and antiplasmin (Merck, Darmstadt, Germany). Urinary and plasma plasminogen concentrations were measured using an ELISA kit (LOXO, Heidelberg, Germany) that detects both plasmin and plasminogen, as indicated by plasmin(ogen). Urinary and plasma aprotinin concentrations were determined using an ELISA kit (Cloud-Clone Corp, Wuhan, China).

Western blots

Expression of γ -ENaC in oocytes and mouse kidney was analyzed using Western blots. Half the kidney per mouse was sliced, and the cortex was dissected using a scalpel. Homogenization was performed using a Dounce homogenisator in 1 ml lysis buffer containing 250 mM sucrose, 10 mM triethanolamine HCl, 1.6 mM ethanolamine, and 0.5

ethylenediamine tetraacetic acid at pH 7.4 (all Sigma-Aldrich, Munich, Germany).³⁷ During all preparation steps, aprotinin (40 µg/ml) and a protease inhibitor cocktail (final concentration 0.1 x stock; cOmplete, Roche Diagnostics, Mannheim, Germany) was present to avoid γ -ENaC cleavage *in vitro*. Homogenates were centrifuged⁴⁵ at 300,000 g for 1 hour, at 4 °C, and the resulting pellet was resuspended and boiled in Laemmli buffer (Sigma-Aldrich, Munich, Germany) at 70 °C for 10 minutes. Subsequently, 40 µg was loaded on a 7.5% polyacrylamide gel for electrophoresis. After transfer to nitrocellulose membranes, the blocked blots were incubated with a custom-made mouse γ -ENaC antibody overnight, at 4 °C, in a 1:500 dilution. This antibody was raised in rabbit against the sequence NTLRLDSAFSSQLTDTQLTNEF, corresponding to the amino acids 634–655 of the C-terminus of murine ENaC (Pineda, Berlin, Germany^{46,47}). For the present study, the obtained antisera were affinity purified as described previously.⁴⁸ Blots were scanned using a fluorescence scanner (Odyssey, LI-COR Biosciences, Lincoln, NE) after incubation with a secondary fluorescent donkey anti-rabbit antibody labelled with IRDye 800CW (LI-COR Biosciences, Lincoln, NE) for 1 hour, at 4 °C, in a 1:20,000 dilution. To test specificity of the obtained bands, the blots were probed with the primary antibody, which was pretreated with the blocking peptide, overnight, or the secondary antibody only. Expression of cadherin was analyzed as a loading control using a goat pan-cadherin antibody (sc-1499, Santa Cruz Biotechnology, Dallas, TX) and a secondary fluorescent donkey anti-goat antibody labelled with IRDye 680RD (LI-COR Biosciences) for 1 hour, at room temperature, in a 1:20,000 dilution. Linearity of the obtained signals was tested by loading various protein amounts (Supplementary Figure S7A and B).

For western blotting of murine γ -ENaC heterologously expressed in *X. laevis* oocytes, a biotinylation approach was used to isolate cell surface proteins as described previously.^{7,11,49} In each group, 30 oocytes expressing murine α -, β -, and γ -ENaC (1 ng of cRNA/subunit of ENaC) were subjected to biotinylation using EZ-Link Sulfo-NHS-SS-Biotin (Thermo Fisher Scientific, Schwerte, Germany). Oocytes were preincubated for 30 minutes, either in ND96 solution (96 mM NaCl, 2 mM KCl, 1 mM CaCl₂, 1 mM MgCl₂, 5 mM Hepes, pH 7.5) or in ND96 solution containing 2 µg/ml chymotrypsin, 500 µg/ml aprotinin, or in both combined. After biotinylation, oocytes were lysed, and proteins were precipitated with Immunopure-immobilized NeutrAvidin beads (Thermo Fisher Scientific, Schwerte, Germany). The lysates were washed with sodium dodecylsulfate polyacrylamide gel electrophoresis sample buffer (Roth, Karlsruhe, Germany), boiled for 5 minutes at 95 °C, and centrifuged for 3 minutes at 20,000 g; the supernatants were then loaded on a 10% sodium dodecylsulfate polyacrylamide gel electrophoresis gel. For detecting γ -ENaC, the anti-mouse γ -ENaC antibody described earlier was used in a 1:1000 dilution. Horseradish peroxidase-labeled secondary goat anti-rabbit antibody (sc-2054, Santa Cruz Biotechnology, Dallas, TX) was used at a 1:50,000 dilution. Chemiluminescence signals were detected using ECL Plus (GE Healthcare, Amersham, United Kingdom).

Quantitative polymerase chain reaction

Transcript levels of α -, β -, and γ -ENaC were analyzed using quantitative real-time polymerase chain reaction analysis with the Light-Cycler System (Roche Life Science, Mannheim, Germany). Kidney tissue from the poles was homogenized using the MagNA Lyser (Roche Life Science, Mannheim, Germany). Cleared cell lysate was transferred for further RNA purification (RNeasy Mini Kit, Qiagen, Hilden, Germany). Next, 1 µg of total RNA was reverse-transcribed to cDNA (BD Biosciences, San Jose, CA) with oligo(dT) primers, according to

the manufacturer's protocol. Transcript levels of the target genes α -, β -, and γ -ENaC; renin; and the housekeeping genes *GAPDH*, β -*actin*, and ribosomal protein 13 (*Rps13*) were determined with the primer pairs in Supplementary Table S4. Polymerase chain reactions were performed with 2 µl cDNA, 2.4 µl MgCl₂ (4 mM), 1 µl primer mix (0.5 µM), 2 µl cDNA Master SYBR Green I mix (Roche Molecular Biochemicals, Mannheim, Germany), and diethylpyrocarbonate-treated water (Advantage RT-for-PCR Kit, Clontech Laboratories, Mountain View, CA), yielding a final volume of 20 µl. Melting point analysis and gel electrophoresis revealed a single product for all target and housekeeping genes. Amplification was in the linear range as analyzed with serial dilutions of the amplicons. Crossing points of the products were determined from the maxima of the second derivative of the signal curve. Absolute copy numbers were calculated, with the serial dilution of the amplicons serving as standards. In addition, expression relative to the housekeeping genes *Rps13* and β -*actin* was calculated using the ΔC_t method.^{50,51} The housekeeping gene *GAPDH* revealed significant variation among the groups and was thus excluded from further analysis (Supplementary Figure S5C). Amplification efficiency as analyzed by conversion of the signal slope was nearly 100%, corresponding to a doubling of the product in each cycle.

Histologic analyses

Expression of γ -ENaC protein from kidneys of healthy, nephrotic, aprotinin- and canrenoate-treated mice were studied 8 days after doxorubicin injection ($n = 2-3$ each) using immunofluorescence microscopy. Paraffin-embedded formalin paraformaldehyde-fixed sections (2 µm) were deparaffinized and rehydrated using standard protocols. Kidney sections were blocked for 45 minutes with normal goat serum diluted 1:5 in 50 mM tris(hydroxymethyl)-aminomethane (Tris), pH 7.4, supplemented with 1% (w/v) skim milk (Bio-Rad Laboratories, Munich, Germany), followed by incubation with the previously mentioned primary antibody (rabbit anti- γ -ENaC, 1:50) for 1 hour, at 37 °C, and subsequent washing in Tris buffer (50 mM Tris, pH 7.4, supplemented with 0.05% (v/v) Tween 20 (Sigma-Aldrich, Munich, Germany; 3 x 5 minutes). Afterward, the secondary antibody (goat anti-rabbit, Invitrogen Alexa Fluor 488, Thermo Fisher Scientific, Schwerte, Germany; 1:200) was applied for 30 minutes. Specificity of the γ -ENaC staining was tested using the primary antibody treated with the blocking peptide overnight. A probe of 11 β -hydroxysteroid dehydrogenase type 2 was conducted with a commercially available sheep anti-11 β -hydroxysteroid dehydrogenase type 2 antibody (AB 1296, Chemicon International, Temecula, CA) and a secondary biotinylated anti-sheep antibody with subsequent detection by Streptavidin Alexa Fluor 568 (Vector Laboratories, Burlingame, CA). To stain nuclei, 4,6-diamidino-2-phenylindole was used (1:1000 in distilled water for 5 minutes), followed by rinsing in Tris buffer (3 x 5 minutes). Finally, sections were covered with Mowiol mounting medium (Calbiochem, La Jolla, CA) and analyzed using laser scanning confocal microscopy (Zeiss LSM 710, Zeiss, Jena, Germany). Staining with γ -ENaC was quantified in hydroxysteroid dehydrogenase type 2--positive distal tubules in 20 high-power fields at 200-fold magnification using a score as follows: 0 (no staining); 1 (weak staining); 2 (marked staining); and 3 (strong staining). Cumulative scores were divided by the number of high-power fields to obtain the final average score value. Scoring was done in an observer-blinded fashion.

Whole-cell current measurements in murine ENaC-expressing oocytes using the 2-electrode voltage-clamp technique

Oocytes were collected from *X. laevis* as described.^{11,49} Defolliculated stage V-VI oocytes were injected with cRNA encoding murine α -, β -,

and γ -ENaC (0.05–0.2 ng of cRNA/subunit of ENaC). Measurement of ENaC-mediated whole-cell currents was completed using the 2-electrode voltage-clamp technique 2 days after cRNA injection as previously described.^{11,49} Chymotrypsin and aprotinin were added as indicated at a concentration of 2 μ g/ml and 500 μ g/ml, respectively. Amiloride-sensitive currents (ΔI_{ami}) were determined by subtracting the current values recorded in the presence of amiloride (2 μ M) from those recorded in the absence of amiloride.

Statistical analyses

Data are provided as arithmetic means \pm SEM, with n representing the number of independent experiments, and N the number of batches of oocytes. Data were tested for normality with the Kolmogorov–Smirnov test, the D’Agostino and Pearson omnibus normality test, and the Shapiro–Wilk test. Variances were tested using the Bartlett test for equal variances. Accordingly, data were tested for significance using parametric or nonparametric analysis of variance, followed by the Dunnett, Dunn, or Tukey multiple comparison posttest, the paired or unpaired Student t -test, or the Mann–Whitney U test where applicable, using GraphPad Prism 6 (GraphPad Software, San Diego, CA). Densitometric analysis of western blots was done using Image Studio, Version 3.1.4 (LI-COR Biosciences, Lincoln, NE). A P value of <0.05 with 2-tailed testing was considered statistically significant.

Study approval

All animal experiments were conducted according to the National Institutes of Health Guide for the Care and Use of Laboratory Animals and the German Law for the Welfare of Animals, and they were approved by local authorities (Regierungspräsidium Tübingen, approval number M5/13). The patient study was conducted in compliance with the Declaration of Helsinki and was approved by the local ethics committee of University Hospital Tübingen (259/2012MPG23).

DISCLOSURE

All the authors declared no competing interests.

ACKNOWLEDGEMENTS

This study was supported by a grant from the German Research Foundation (DFG, AR 1092/2-1). The authors acknowledge the expert technical assistance of Antje Raiser, Melanie Märklin, PhD, Manfred Depner, and Christina Lang.

SUPPLEMENTARY MATERIAL

Figure S1. Characteristics of experimental nephrotic syndrome in 129S1/SvImJ mice. Nephrotic mice developed ascites (A, upper panel) and visible lipemia (B, right side). Note the reduced hematocrit ratio as a correlate of volume retention. Although food and fluid intake remained fairly constant (C), a marked renal sodium avidity is indicated by a fall in the urinary Na/K ratio (D). Arithmetic means \pm SEM. # indicates a significant difference from baseline value.

Figure S2. Inhibition curves for amidolytic activity with purified active plasmin. Pooled curve from $n = 5$ –7 single curves, using a final plasmin concentration in the well of 27 μ g/ml.

Figure S3. Food and fluid intake (A,B), as well as renal sodium avidity indicated by the urinary Na/K ratio (C), during treatment with pellets containing placebo, aprotinin, camostat, and tranexamic acid, respectively. Arithmetic means \pm SEM. # indicates a significant difference from baseline value; * indicates a significant difference between placebo- and aprotinin-treated mice. d, days.

Figure S4. Effect of high salt intake on aldosterone secretion and volume retention in healthy and nephrotic mice. In healthy mice, body weight (bw) remained stable under high salt (hs) intake with 1% NaCl in the drinking water, whereas aldosterone secretion was significantly suppressed. After injection of doxorubicin and onset of proteinuria nephrotic mice treated with placebo (plac) pellets developed marked volume retention, and plasma aldosterone concentration remained suppressed. Aprotinin (aprot) treatment prevented bw gain completely. This longitudinal experiment indicates that proteinuria confers salt sensitivity to formerly salt-insensitive mice, which is independent from aldosterone and relates to urinary excretion of aprotinin-sensitive serine proteases (A). Plasma aldosterone concentration at day 10 after doxorubicin injection and maximal (max.) bw gain during various treatments (amil = amiloride; can = canrenoate; cam = camostat; txa = tranexamic acid). Note the pattern difference in the 2 parameters (B). Arithmetic means \pm SEM. # indicates a significant difference from baseline value; * indicates a significant difference between placebo- and aprotinin-treated mice.

Figure S5. Graph showing mRNA expression of renin and the housekeeping genes, in healthy and nephrotic mice. Absolute mRNA expression of renin in healthy, placebo, and aprotinin (aprot)-treated nephrotic mice ($n = 8$ –9 each; A). Relative mRNA expression of renin normalized to the housekeeping gene β -actin in healthy, placebo-, and aprotinin-treated nephrotic mice ($n = 8$ –9 each; B). Absolute mRNA expression of the housekeeping genes *GAPDH*, *Rps13*, and β -actin in healthy, placebo-treated nephrotic and aprotinin-treated nephrotic mice ($n = 8$ –9 each). Note that *GAPDH* expression is significantly decreased in aprotinin-treated nephrotic mice (C). Arithmetic means \pm SEM. # indicates a significant difference from baseline value; * indicates a significant difference between placebo- and aprotinin-treated mice.

Figure S6. Expression of epithelial sodium channel (ENaC) subunits in healthy and nephrotic mice. Absolute mRNA expression of the α -, β -, and γ -subunit of ENaC in healthy mice, placebo-treated nephrotic mice, and aprotinin-treated nephrotic mice ($n = 8$ –9 each; A). Relative mRNA expression of the α -, β -, and γ -subunit of ENaC normalized to the housekeeping gene β -actin in healthy mice, placebo-treated nephrotic mice, and aprotinin-treated nephrotic mice ($n = 8$ –9 each). # indicates a significant difference from healthy mice (B); * indicates a significant difference between placebo- and aprotinin-treated nephrotic mice.

Figure S7. Expression of γ -epithelial sodium channel (γ -ENaC) in renal cortex analyzed using Western blot. Western blot from renal cortex demonstrating linearity of the signal obtained for the expression of the loading control cadherin and the γ -ENaC bands at 53, 70, and 86 kDa (A,B).

Figure S8. Semiquantitative analysis and specificity of γ -epithelial sodium channel (γ -ENaC) staining in the aldosterone-sensitive distal nephron. Cross-sections at 200-fold magnification were analyzed using a staining score (0 = none; 1 = weak; 2 = marked; 3 = strong) in healthy and nephrotic mice treated with placebo or aprotinin (aprot) ($n = 2$ –3 each; $N =$ total number of analyzed high-power fields). Immunofluorescence using the primary γ -ENaC antibody in the presence of the blocking peptide (B). # indicates a significant difference from healthy mice, * indicates a significant difference between placebo- and aprotinin-treated nephrotic mice.

Figure S9. Aprotinin (aprot) prevents proteolytic activation of epithelial sodium channel (ENaC) by chymotrypsin (chy), and preincubation with aprot has no effect on baseline amiloride-sensitive currents ΔI_{ami} (amiloride). Representative whole-cell current traces from oocytes expressing murine ENaC. Amiloride (2 μ M), chy (2 μ g/ml) $-/+$ aprot (500 μ g/ml) (chy + aprot) were present in the bath solution as indicated (A,B). Summary of similar experiments as shown in the representative traces. Data points obtained from individual oocytes are connected by a line (C). Oocytes expressing murine ENaC were preincubated for 48 hours with and without aprotinin (500 μ g/ml). To pool

data from different batches of oocytes, individual ΔI_{ami} values were normalized to the mean ΔI_{ami} value of the control group (- chy; D). N indicates the number of different batches of oocytes. # indicates a significant difference between indicated groups. I, flow or current; ns, nonsignificant.

Table S1. Calculated IC_{50} values and comparison between urinary amidolytic and plasmin activity.

Table S2. Patient characteristics, fluid status, and urinary amidolytic activity. Data are given as medians with interquartile range. GFR, glomerular filtration rate.

Table S3. Number of included and excluded mice.

Table S4. Used primers. bp, base pair.

Supplementary References.

Supplementary material is linked to the online version of the paper at www.kidney-international.org.

REFERENCES

- Bockenbauer D. Over- or underfill: not all nephrotic states are created equal. *Pediatr Nephrol (Berlin, Germany)*. 2013;28:1153–1156.
- Deschênes G, Wittner M, Stefano A, et al. Collecting duct is a site of sodium retention in PAN nephrosis: a rationale for amiloride therapy. *J Am Soc Nephrol*. 2001;12:598–601.
- Palmer LG, Frindt G. Regulation of epithelial Na channels by aldosterone. *Kitasato Med J*. 2016;46:1–7.
- Rossier BC, Stutts MJ. Activation of the epithelial sodium channel (ENaC) by serine proteases. *Annu Rev Physiol*. 2009;71:361–379.
- Passero CJ, Hughey RP, Kleyman TR. New role for plasmin in sodium homeostasis. *Curr Opin Nephrol Hypertens*. 2010;19:13–19.
- Siddall EC, Radhakrishnan J. The pathophysiology of edema formation in the nephrotic syndrome. *Kidney Int*. 2012;82:635–642.
- Svenningsen P, Bistrup C, Friis UG, et al. Plasmin in nephrotic urine activates the epithelial sodium channel. *J Am Soc Nephrol*. 2009;20:299–310.
- Buhl KB, Friis UG, Svenningsen P, et al. Urinary plasmin activates collecting duct ENaC current in preeclampsia. *Hypertension*. 2012;60:1346–1351.
- Svenningsen P, Andersen H, Nielsen LH, Jensen BL. Urinary serine proteases and activation of ENaC in kidney—implications for physiological renal salt handling and hypertensive disorders with albuminuria. *Pflügers Arch*. 2015;467:531–542.
- Passero CJ, Mueller GM, Rondon-Berrios H, et al. Plasmin activates epithelial Na⁺ channels by cleaving the gamma subunit. *J Biol Chem*. 2008;283:36586–36591.
- Haerteis S, Krappitz M, Diakov A, et al. Plasmin and chymotrypsin have distinct preferences for channel activating cleavage sites in the γ subunit of the human epithelial sodium channel. *J Gen Physiol*. 2012;140:375–389.
- Andersen H, Friis UG, Hansen PB, et al. Diabetic nephropathy is associated with increased urine excretion of proteases plasmin, prostaticin and urokinase and activation of amiloride-sensitive current in collecting duct cells. *Nephrol Dial, Transplant*. 2015;30:781–789.
- Buhl KB, Oxlund CS, Friis UG, et al. Plasmin in urine from patients with type 2 diabetes and treatment-resistant hypertension activates ENaC *in vitro*. *J Hypertens*. 2014;32:1672–1677; discussion 1677.
- Schorck A, Woern M, Kalbacher H, et al. Association of plasminuria with overhydration in patients with CKD. *Clin J Am Soc Nephrol*. 2016;11:761–769.
- Rajj L, Tian R, Wong JS, et al. Podocyte injury: the role of proteinuria, urinary plasminogen, and oxidative stress. *Am J Physiol Renal Physiol*. 2016;311:F1308–F1317.
- Makino H, Onbe T, Kumagai I, et al. A proteinase inhibitor reduces proteinuria in nephrotic syndrome. *Am J Nephrol*. 1991;11:164–165.
- Onbe T, Makino H, Kumagai I, et al. Effect of proteinase inhibitor camostat mesilate on nephrotic syndrome with diabetic nephropathy. *J Diabet Complications*. 1991;5:167–168.
- Maekawa A, Kakizoe Y, Miyoshi T, et al. Camostat mesilate inhibits prostaticin activity and reduces blood pressure and renal injury in salt-sensitive hypertension. *J Hypertens*. 2009;27:181–189.
- Uchimura K, Kakizoe Y, Onoue T, et al. *In vivo* contribution of serine proteases to the proteolytic activation of γ ENaC in aldosterone-infused rats. *Am J Physiol Renal Physiol*. 2012;303:F939–F943.
- Midgley I, Hood AJ, Proctor P, et al. Metabolic fate of 14C-camostat mesylate in man, rat and dog after intravenous administration. *Xenobiotica*. 1994;24:79–92.
- Zheng H, Liu X, Sharma NM, et al. Urinary proteolytic activation of renal epithelial Na⁺ channels in chronic heart failure. *Hypertension*. 2016;67:197–205.
- Artunc F, Nasir O, Amann K, et al. Serum- and glucocorticoid-inducible kinase 1 in doxorubicin-induced nephrotic syndrome. *Am J Physiol Renal Physiol*. 2008;295:F1624–F1634.
- Bohnert BN, Daniel C, Amann K, et al. Impact of phosphorus restriction and vitamin D-substitution on secondary hyperparathyroidism in a proteinuric mouse model. *Kidney Blood Press Res*. 2015;40:153–165.
- Beath SM, Nuttall GA, Fass DN, et al. Plasma aprotinin concentrations during cardiac surgery: full- versus half-dose regimens. *Anesth Analg*. 2000;91:257–264.
- Kim SW, Wang W, Nielsen J, et al. Increased expression and apical targeting of renal ENaC subunits in puromycin aminonucleoside-induced nephrotic syndrome in rats. *Am J Physiol Renal Physiol*. 2004;286:F922–F935.
- Haerteis S, Krueger B, Korbmacher C, Rauh R. The delta-subunit of the epithelial sodium channel (ENaC) enhances channel activity and alters proteolytic ENaC activation. *J Biol Chem*. 2009;284:29024–29040.
- Korbmacher C, Mansley MK, Bertog M. Activation of the epithelial sodium channel (ENaC) by aldosterone in mCCD_{cl1} mouse renal cortical collecting duct cells is dependent on SGK1 and can be prevented by inhibiting endogenous proteases. *FASEB J*. 2017;31(856):5.
- Carattino MD, Mueller GM, Palmer LG, et al. Prostaticin interacts with the epithelial Na⁺ channel and facilitates cleavage of the γ -subunit by a second protease. *Am J Physiol Renal Physiol*. 2014;307:F1080–F1087.
- Patel AB, Chao J, Palmer LG. Tissue kallikrein activation of the epithelial Na channel. *Am J Physiol Renal Physiol*. 2012;303:F540–F550.
- Svenningsen P, Uhrenholt TR, Palarasah Y, et al. Prostaticin-dependent activation of epithelial Na⁺ channels by low plasmin concentrations. *Am J Physiol Regul Integr Comp Physiol*. 2009;297:R1733–R1741.
- Yu JX, Chao L, Chao J. Prostaticin is a novel human serine proteinase from seminal fluid. Purification, tissue distribution, and localization in prostate gland. *J Biol Chem*. 1994;269:18843–18848.
- Levy Yeyati N, Fellet A, Arranz C, et al. Amiloride-sensitive and amiloride-insensitive kaliuresis in advanced chronic kidney disease. *J Nephrol*. 2008;21:93–98.
- Chiu TF, Bullard MJ, Chen JC, et al. Rapid life-threatening hyperkalemia after addition of amiloride HCl/hydrochlorothiazide to angiotensin-converting enzyme inhibitor therapy. *Ann Emerg Med*. 1997;30:612–615.
- Whiting GF, McLaran CJ, Bochner F. Severe hyperkalaemia with Moduretic. *Med J Aust*. 1979;1:409.
- Jaffey L, Martin A. Malignant hyperkalaemia after amiloride/hydrochlorothiazide treatment. *Lancet*. 1981;2:1272.
- Mangano DT, Tudor IC, Dietzel C, Multicenter Study of Perioperative Ischemia Research Group; Ischemia Research and Education Foundation. The risk associated with aprotinin in cardiac surgery. *New Engl J Med*. 2006;354:353–365.
- Yang L, Frindt G, Lang F, et al. SGK1-dependent ENaC processing and trafficking in mice with high dietary K intake and elevated aldosterone. *Am J Physiol Renal Physiol*. 2017;312:F65–F76.
- Kleyman TR, Carattino MD, Hughey RP. ENaC at the cutting edge: regulation of epithelial sodium channels by proteases. *J Biol Chem*. 2009;284:20447–20451.
- Frindt G, Ergonul Z, Palmer LG. Surface expression of epithelial Na channel protein in rat kidney. *J Gen Physiol*. 2008;131:617–627.
- Patel AB, Frindt G, Palmer LG. Feedback inhibition of ENaC during acute sodium loading *in vivo*. *Am J Physiol Renal Physiol*. 2013;304:F222–F232.
- de Seigneux S, Kim SW, Hemmingsen SC, et al. Increased expression but not targeting of ENaC in adrenalectomized rats with PAN-induced nephrotic syndrome. *Am J Physiol Renal Physiol*. 2006;291:F208–F217.
- Jacquillet G, Chichger H, Unwin RJ, Shirley DG. Protease stimulation of renal sodium reabsorption *in vivo* by activation of the collecting duct epithelial sodium channel (ENaC). *Nephrol Dial Transplant*. 2013;28:839–845.
- Lourdel S, Loffing J, Favre G, et al. Hyperaldosteronemia and activation of the epithelial sodium channel are not required for sodium retention in puromycin-induced nephrosis. *J Am Soc Nephrol*. 2005;16:3642–3650.
- Artunc F, Ebrahim A, Siraskar B, et al. Responses to diuretic treatment in gene-targeted mice lacking serum- and glucocorticoid-inducible kinase 1. *Kidney Blood Press Res*. 2009;32:119–127.
- Picard N, Eladari D, El Moghrabi S, et al. Defective ENaC processing and function in tissue kallikrein-deficient mice. *J Biol Chem*. 2008;283:4602–4611.

46. Nesterov V, Krueger B, Bertog M, et al. In Liddle syndrome, epithelial sodium channel is hyperactive mainly in the early part of the aldosterone-sensitive distal nephron. *Hypertension*. 2016;67:1256–1262.
47. Krueger B, Haerteis S, Yang L, et al. Cholesterol depletion of the plasma membrane prevents activation of the epithelial sodium channel (ENaC) by SGK1. *Cell Physiol Biochem*. 2009;24:605–618.
48. Vallur R, Kalbacher H, Feil R. Catalytic activity of cGMP-dependent protein kinase type I in intact cells is independent of N-terminal autophosphorylation. *PLoS One*. 2014;9:e98946.
49. Haerteis S, Krappitz A, Krappitz M, et al. Proteolytic activation of the human epithelial sodium channel by trypsin IV and trypsin I involves distinct cleavage sites. *J Biol Chem*. 2014;289:19067–19078.
50. Livak KJ, Schmittgen TD. Analysis of relative gene expression data using real-time quantitative PCR and the 2(-Delta Delta C(T)) Method. *Methods*. 2001;25:402–408.
51. Wagner CA, Loffing-Cueni D, Yan Q, et al. Mouse model of type II Bartter's syndrome. II. Altered expression of renal sodium- and water-transporting proteins. *Am J Physiol Renal Physiol*. 2008;294:F1373–F1380.